Structural and transport properties of $Sr_2VO_{3-\delta}FeAs$ superconductors with different oxygen deficiencies

Fei Han, Xiyu Zhu, Gang Mu, Peng Cheng, Bing Shen, Bin Zeng and Hai-Hu Wen*
National Laboratory for Superconductivity, Institute of Physics and Beijing National Laboratory for Condensed Matter Physics, Chinese Academy of Sciences, P. O. Box 603, Beijing 100190, China

$Sr_2VO_{3-\delta}FeAs$ superconductors with different oxygen deficiencies have been successfully fabricated. It is found that the superconducting transition temperature drops down monotonically with the increase of oxygen deficiency. The diminishing of superconductivity is accompanied by the enhancement of residual resistivity, indicating an unraveled scattering effect induced by the oxygen deficiency. The highest superconducting transition temperature at about 40 K is achieved near the stoichiometrical sample Sr_2VO_3FeAs. Surprisingly, the X-ray photoelectron spectroscopy (XPS) shows that the vanadium has a "5+" valence state in the samples. The Hall effect measurements reveal that the density of charge carriers (electron-like here) varies qualitatively with the increase of oxygen deficiency. Magnetotransport measurements show that the superconducting transition changes from one-step-like shape at low fields to two-step-like one at high fields, indicating a high anisotropy.

PACS numbers: 74.70.Dd, 74.25.Fy, 75.30.Fv, 74.10.+v

I. INTRODUCTION

The iron-based superconductors have formed a new family in the field of high-T_c superconductivity.[1,2] Very soon, many new structures with the FeAs layers have been found, including the so-called 1111 phase (LNFeAsO, AEFeAsF, LN = rare earth elements, AE = alkaline earth elements),[1,3,4] 122 phase ($AEFe_2As_2$, AE = alkaline earth elements),[5,6,7] 111 phase (LiFeAs, NaFeAs),[8,9] and 11 phase (FeSe).[10] Inspired by the experience in the cuprates, a higher T_c can be achieved in a system with an expanded c-axis lattice, therefore, to explore new systems with much expanded c-axis lattice constants is highly desired. Towards this direction, the FeAs-based compound $Sr_3Sc_2O_5Fe_2As_2$ with perovskite structure was found by our group.[11] Unfortunately no superconductivity was found in this compound. Later on, a new FeP-base compound Sr_2ScO_3FeP with perovskite structure has been found and shown to be a new superconductor at 17 K.[12] Recently, we successfully fabricated a new superconductor Sr_2VO_3FeAs with $T_c = 37.2$ K.[13] By applying a high pressure to Sr_2VO_3FeAs, the T_c has been raised to 46 K.[14] Several theoretical interests were raised on this interesting superconductor. It was suggested that both Fe and V contribute quasiparticle density of states (DOS) at the Fermi energy E_F, while the electrons from the vanadium are 100% spin polarized.[15] Also based on the band structure calculation, Lee and Pickett concluded that the Fe-derivative orbitals do not have the nesting condition,[16] therefore the model of superconductivity mechanism based on the interpocket scattering of electrons through exchanging anti-ferromagnetic spin fluctuations was questioned. Recently it was argued that the nesting condition of Fe-derivative bands may still hold in this material, although the nesting condition is not as good as in other systems.[17] Therefore in this system, there are several important questions to be answered: (1) Whether the superconductivity is induced by the oxygen deficiency or multivalence state of vanadium? (2) Is the system really a highly anisotropic one as expected from the structure parameters? (3) Is there a nesting condition for the Fermi surfaces of the Fe-derivative bands or not? In this paper, we report the fabrication and characterization of the superconducting system $Sr_2VO_{3-\delta}FeAs$ with different oxygen contents.

II. EXPERIMENTAL

By using the solid state reaction method,[18] we successfully fabricated the superconducting system $Sr_2VO_{3-\delta}FeAs$ with different oxygen contents. Firstly, FeAs, and SrAs powders were obtained by the chemical reaction method with Fe powders (purity 99.99%), Sr pieces (purity 99.9%) and As grains (purity 99.999%). Then they were mixed with V_2O_3 (purity 99.9%), SrO (purity 99%), and Fe powders (purity 99.99%) in the formula $Sr_2VO_{3-\delta}FeAs$, ground and pressed into a pellet shape. All the weighing, mixing and pressing procedures were performed in a glove box with a protective argon atmosphere (both H_2O and O_2 are limited below 0.1 ppm). The pellet was sealed in a silica tube under 0.2 atm argon atmosphere and followed by a heat treatment at 1050 ^oC for 30 hours. Then it was cooled down slowly to room temperature. The X-ray diffraction (XRD) patterns of our samples were carried out by a *Mac-Science* MXP18A-HF equipment with $\theta-2\theta$ scan. The XRD data taken on powder samples was analyzed by the Rietveld fitting method using the GSAS suite.[19] The DC susceptibility of the samples was measured on a superconducting quantum interference device (SQUID, MPMS-7T) of Quantum Design. The resistivity and Hall effect measurements were done using a six-probe technique on the Quantum Design instrument physical property measure-

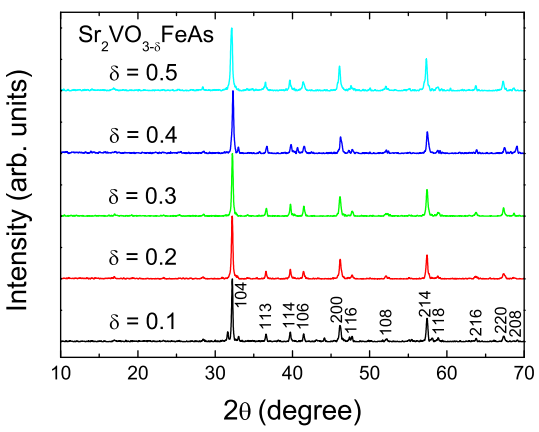

FIG. 1: (Color online) X-ray diffraction patterns for the samples $Sr_2VO_{3-\delta}FeAs$. One can see that all the main peaks can be indexed to the structure of FeAs-21311 with the space group of *P4/nmm*.

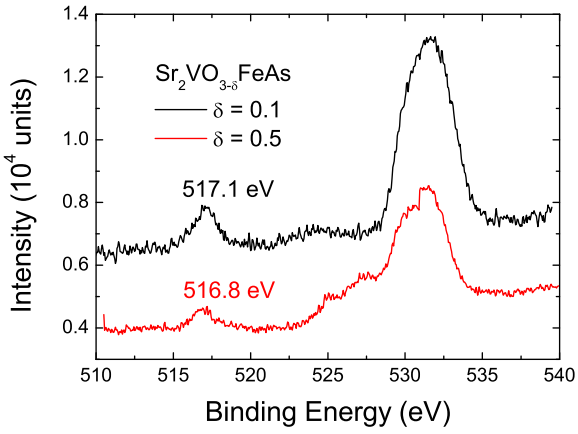

FIG. 2: (Color online) The X-ray photoelectron spectroscopy (XPS) on $Sr_2VO_{3-\delta}FeAs$.

ment system with magnetic fields up to 9 T (PPMS-9T). The temperature stabilization was better than 0.1% and the resolution of the voltmeter was better than 10 nV.

III. RESULTS AND DISCUSSION

A. Superconductivity tuned by oxygen deficiency

In Fig. 1, we present the x-ray diffraction (XRD) patterns of the compounds $Sr_2VO_{3-\delta}FeAs$ with δ from 0.1 to 0.5. These compounds contain a stacking of anti-fluorite (Fe_2As_2) layers and perovskite-type ($Sr_4V_2O_6$) layers. For these samples, all the main peaks can be indexed to the tetragonal structure with the space group *P4/nmm*. The impurity phase was found to come from Sr_2VO_4. It is found that the lattice constants change only slightly upon the change of oxygen content. Taking $Sr_2VO_{2.5}FeAs$ as an example, the lattice constants were determined to be a = 3.927$\AA$ and c = 15.666$\AA$, while a = 3.928$\AA$ and c = 15.669$\AA$ for $Sr_2VO_{2.9}FeAs$. Comparing the two samples, we may conclude that although the oxygen contents of these samples change a lot, but the structure will relax by itself and the lattice constants change slightly.

As we know, the vanadium in the perovskite structure has multiple valence states. For example, the vanadium has a valence state of "3+" in the $LaSrVO_4$, while that in Sr_2VO_4 is "4+". In order to determine the valence states of our samples, we measured the X-ray photoelectron spectroscopy (XPS) of the samples $Sr_2VO_{3-\delta}FeAs$ with $\delta = 0.1$, 0.5, as shown in Fig. 2. As we can see, there are peeks at about 517 eV which means the vanadium may be on "5+" valence state in the samples. With reducing oxygen content, the main peak of vanadium shifts slightly from 517.1 eV to 516.8 eV, suggesting that the vanadium has a quite stable valence state. The V^{5+} state is however unexpected by a simple counting on the electrons. Assuming that the (FeAs) has a "-1" valence state, and the cationic state Sr^{2+} and O^{2-}, we then have two electrons doped to each (FeAs). This is a highly doped state compared to that in $LaFeAsO_{1-x}F_x$ and $Ba(Fe_{1-x}Co_x)_2As_2$. However as we know the XPS detects only the valence state on the surface layer, so we cannot conclude definitely that the vanadium is at a valence state of "5+" in the interior part of the samples. Future experiments are strongly desired to resolve this puzzle. It may be safe to conclude that the superconductivity achieved in $Sr_2VO_{3-\delta}FeAs$ is because the vanadium contributes large amount of electrons to the (FeAs) planes.

Although the lattice constants and the valence state of vanadium do not exhibit a clear change with the oxygen deficiency, the superconductivity property is however strongly influenced. In Fig. 3, we show the temperature dependence of DC magnetization for $Sr_2VO_{3-\delta}FeAs$ with δ from 0.1 to 0.5. The measurements were carried out under a magnetic field of 20 Oe in zero-field-cooled and field-cooled processes. As we can see, the superconducting transition temperature drops with the increase of oxygen deficiency. When δ is 0.1, 0,2, and 0.3, the diamagnetization signal is quite big. While δ is up to 0.4, 0.5, the diamagnetization signal becomes very small. One possible reason is that there is a very weak superfluid density when plenty of the Cooper pairs are broken by the disorders induced by oxygen deficiencies.

We also present the electrical resistance of the samples $Sr_2VO_{3-\delta}FeAs$ normalized to their values at 300 K in Fig. 4. As we can see the superconducting transition temperature drops down monotonically with the increase of oxygen deficiency. The superconducting transition temperature was about 20 K for $\delta = 0.5$, while it was about 40 K with $\delta = 0.1$. It is clear that there is an apparent change of behavior from a good metal to

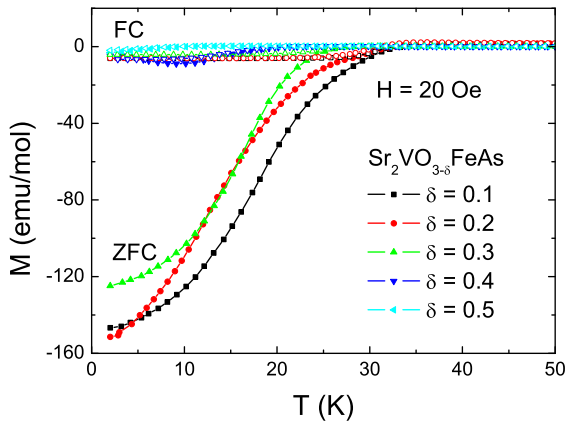

FIG. 3: (Color online) Temperature dependence of DC magnetization for the samples $Sr_2VO_{3-\delta}FeAs$. The DC susceptibility data was obtained using the zero-field-cooling and field-cooling modes under a magnetic field of 20 Oe. For the oxygen deficient samples with $\delta = 0.4$, 0.5, the diamagnetization signal is much weaker than the others.

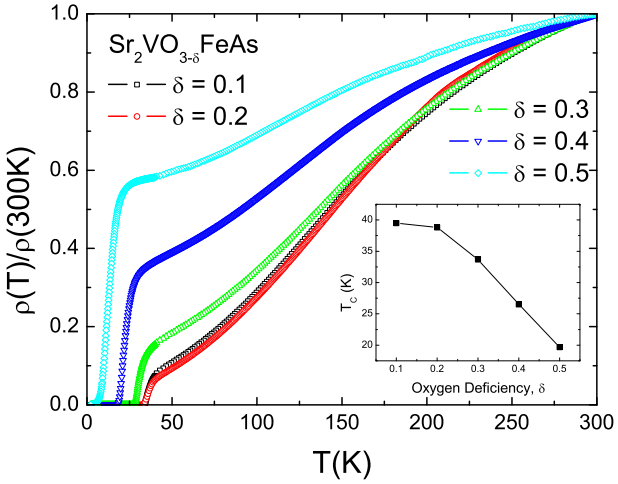

FIG. 4: (Color online) Electrical resistance of $Sr_2VO_{3-\delta}FeAs$ normalized to its value at 300K.The transition temperature drops monotonically with the increase of oxygen deficiency. The inset show the doping dependence of superconducting transition temperature T_c. The highest superconducting transition temperature is achieved near the stoichiometric formula $Sr_2VO_{2.9}FeAs$.

a bad metal. As we can see the residual resistance ratio $RRR \equiv \rho(300\ \mathrm{K})/\rho(30\ \mathrm{K})$ changes from about 14 to about 1.7 when δ varies from 0.1 to 0.5. For the sample with $\delta = 0.5$, the residual resistivity becomes very big. This may be understood that the electron conduction contributed by the vanadium is strongly suppressed by the oxygen deficiency. An alternative way to understand the large residual resistivity for this oxygen deficient sample is that the oxygen deficiency leads to an enhanced electrons scattering in the (FeAs) planes: The local oxygen deficiency will twist the V-O semi-octahedron leading to a severe influence on the local structure of the (FeAs) quasi 2D planes. It remains unclear why the transition temperature drops sharply with the increase of oxygen deficiency. We believe there is a close relationship between the suppression of superconducting transition temperature and the enhancement of residual resistivity. We thus naturally conclude that the pair breaking effect caused by disorders (as evidenced by the stronger residual resistivity) may be the reason for the suppression of superconductivity. The inset of Fig. 4 shows the doping dependence of the transition temperature T_c. One can see that the highest Tc is achieved at the stoichiometric formula $Sr_2VO_{2.9}FeAs$. Therefore naturally we conclude that the superconductivity in the present system is not induced by the oxygen deficiency.

B. Hall effect

In order to investigate how the oxygen deficiency influences the superconducting behavior, we measured the Hall effect in the normal state with $\delta = 0.1$, 0.3, 0.5. Fig. 5(a)-5(c) show the magnetic field dependence of Hall resistivity (ρ_{xy}) at different temperatures. In the experiment, ρ_{xy} was taken as $\rho_{xy} = [\rho(+H) - \rho(-H)]/2$ at each point to eliminate the effect of the misaligned Hall electrodes. The raw data of the transverse resistivity ρ_{xy} are all negative and exhibits a linear relation with the magnetic field. This is similar to that in other FeAs-based superconductors.[18] Fig. 5(d) shows the negative Hall coefficients $R_H = \rho_{xy}/H$ of the three samples. As we can see, the absolute Hall coefficient drops with the increase of oxygen deficiency, which means that the density of electron-like charge carriers drops with the decrease of oxygen deficiency. The strong temperature dependent behavior of the Hall coefficient R_H suggests either a strong multi-band effect or a spin related scattering effect. It is interesting to note that the sample with higher T_c has a weaker temperature dependence of R_H. This is similar to that in other systems. For example, in $LaFeAsO_{1-x}F_x$, much weaker temperature dependence is observed for the optimally doped sample. While the R_H of the underdoped sample exhibits a very strong temperature dependence.

C. High anisotropy of superconductivity

In Fig. 6(a)-6(c) we present the temperature dependence of resistivity for the samples $Sr_2VO_{3-\delta}FeAs$ ($\delta = 0.1$, 0.3, 0.5) under different magnetic fields. The onset transition temperature of superconductivity is very robust against the magnetic field, just like other iron-pnictide superconductors. As we can see, the superconducting transition evolves from one-step-like at low

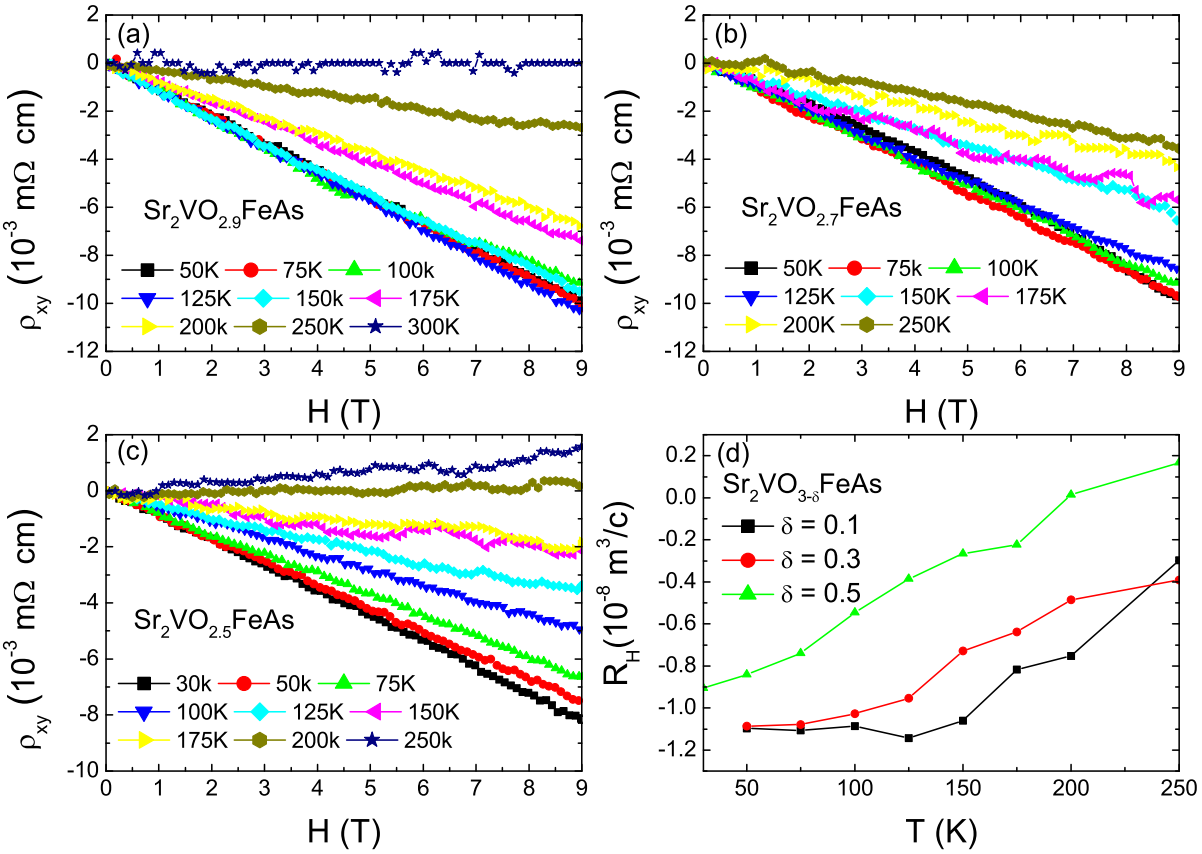

FIG. 5: (Color online) (a)-(c) The Hall resistivity ρ_{xy} versus the magnetic field $\mu_0 H$ at different temperatures for $Sr_2VO_{3-\delta}FeAs$. (d) The absolute Hall coefficient drops down with the increase of oxygen deficiency.

fields to two-step-like at high fields. The second step at a lower temperature may be caused by the inter-layer coupling. This feature has not been found in the other iron-pnictide superconductors. Actually, it was often observed in the highly anisotropic systems in cuprate superconductors like Bi-2212 and Bi-2223. So we suppose the inter-layer coupling field may play an important role here. We used the criterion of $95\%\rho_n$ to determine the upper critical field and show the data in Fig. 6(d), and taking the criterion of $0.1\%\rho_n$ for the irreversibility line H_{irr}. Furthermore we got $(dH_{c2}/dT)_{T_c} \approx$ -12.19 T/K for $\delta = 0.1$, $(dH_{c2}/dT)_{T_c} \approx$ -11.23 T/K for $\delta = 0.3$, and $(dH_{c2}/dT)_{T_c} \approx$ -9.09 T/K for $\delta = 0.5$. These values are rather large which indicates rather high upper critical fields in these systems. In order to determine the upper critical field in the low temperature region, we adopted the Werthamer-Helfand-Hohenberg (WHH) formula $H_{c2} = -0.69(dH_{c2}/dT)_{T_c}T_c$.[20] Finally we get $H_{c2}(0) = 337$ T for $\delta = 0.1$, 283 T for $\delta = 0.3$ and 119 T for $\delta = 0.5$. As we can see there are large regions between the upper critical $H_{c2}(T)$ and the irreversibility field $H_{irr}(T)$. This region may correspond to the vortex liquid region dominated by the motion of pancake vortices. The global shape of vortex phase suggests a high anisotropy of the system. An exact evaluation on the anisotropy of this system would rely on the data measured from single crystals, which is actually underway.

IV. CONCLUSIONS

We have successfully fabricated the superconducting systems $Sr_2VO_{3-\delta}FeAs$ with different oxygen deficiencies. It is found that the lattice constants and the valence state of vanadium do not change with the oxygen deficiency, while the superconducting transition temperature drops down dramatically accompanied by the strong enhancement of the residual resistivity. The highest superconducting transition temperature at about 40 K was achieved near the stoichiometrical sample Sr_2VO_3FeAs, therefore we conclude that the superconductivity in the present sample is not induced by the oxygen deficiency and the multi-valence state. Magnetotransport measurements lead to the determination of the vortex phase di-

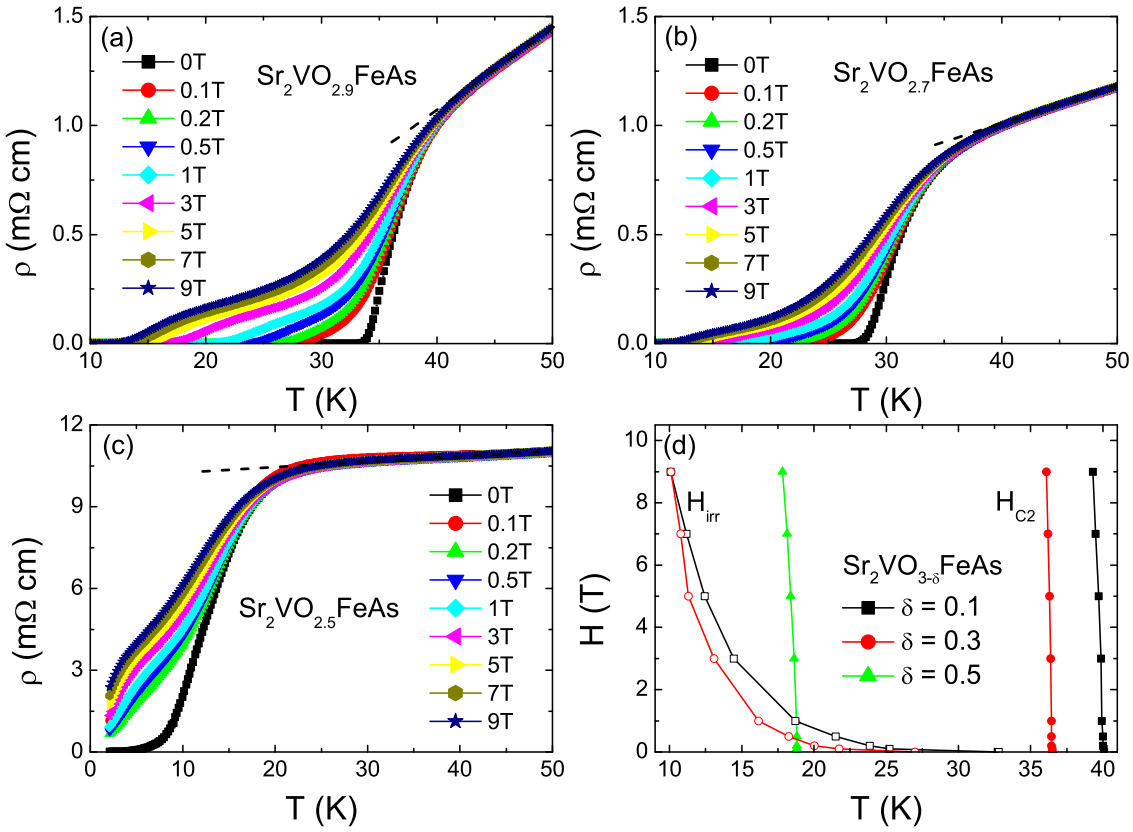

FIG. 6: (Color online) (a)-(c) Temperature dependence of resistivity in the low temperature region under different magnetic fields for $Sr_2VO_{3-\delta}FeAs$. (d) The phase diagram plotted as H versus T. A criterion of $95\%\rho_n$ was taken to determine the upper critical fields, $0.1\%\rho_n$ for the irreversibility line H_{irr}. One can see that the one-step transition at a low field will evolve into a two-step transition at a high field.

agram which resembles to that of highly anisotropic system, such as Bi-2212 and Bi-2223. Hall effect measurements clearly indicate a multi-band feature of the electron conduction.

V. ACKNOWLEDGEMENTS

This work was supported by the Natural Science Foundation of China, the Ministry of Science and Technology of China (973 Projects No.2006CB601000, No. 2006CB921802), and Chinese Academy of Sciences (Project ITSNEM).

* Electronic address: hhwen@aphy.iphy.ac.cn

[1] Y. Kamihara, T. Watanabe, M. Hirano, and H. Hosono, J. Am. Chem. Soc. **130**, 3296 (2008).
[2] H. H. Wen, Adv. Mater. **20**, 3764-3769 (2008).
[3] S. Matsuishi, Y. Inoue, T. Nomura, H. Yanagi, M. Hirano, and H. Hosono, J. Am. Chem. Soc. **130**, 14428 (2008).
[4] F. Han, X. Zhu, G. Mu, P. Cheng, and H. H. Wen, Phys. Rev. B **78**, 180503(R) (2008).
[5] M. Rotter, M. Tegel, and D. Johrendt, Phys. Rev. Lett. **101**, 107006 (2008).
[6] K. Sasmal, B. Lv, B. Lorenz, A. M. Guloy, F. Chen, Y. Y. Xue, and C. W. Chu, Phys. Rev. Lett. **101**, 107007 (2008).
[7] A. S. Sefat, R. Jin, M. A. McGuire, B. C. Sales, D. J. Singh, and D. Mandrus, Phys. Rev. Lett. **101**, 117004 (2008).

[8] X. C. Wang, Q. Q. Liu, Y. X. Lv, W. B. Gao, L. X. Yang, R. C. Yu, F. Y. Li, and C. Q. Jin, Solid State Commun. **148** 538 (2008).
[9] J. H. Tapp, Z. Tang, B. Lv, K. Sasmal, B. Lorenz, P. C. W. Chu, and A. M. Guloy, Phys. Rev. B **78**, 060505(R) (2008).
[10] F. C. Hsu, J. Y. Luo, K. W. Yeh, T. K. Chen, T. W. Huang, P. M. Wu, Y. C. Lee, Y. L. Huang, Y. Y. Chu, D. C. Yan, and M. K. Wu, Proc. Natl. Acad. Sci. **105**, 14262 (2008).
[11] X. Zhu, F. Han, G. Mu, B. Zeng, P. Cheng, B. Shen, and H. H. Wen, Phys. Rev. B **79**, 024516 (2009).
[12] H. Ogino, Y. Matsumura, Y. Katsura, K. Ushiyama, S. Horii, K. Kishio, and J. Shimoyama, Supercond. Sci. Technol. **22**, 075008 (2009).
[13] X. Zhu, F. Han, G. Mu, P. Cheng, B. Shen, B. Zeng, and H. H. Wen, Phys. Rev. B **79**, 220512(R) (2009).
[14] H. Kotegawa, T. Kawazoe, H. Tou, K. Murata, H. Ogino, K. Kishio, and J. Shimoyama, arXiv:condmat/0908.1469 (2009).
[15] I. R. Shein, and A. L. Ivanovskii, J. Supercond. Nov. Magn. **22**, 613-617 (2009).
[16] K. W. Lee, and W. E. Pickett, arXiv:condmat/0908.2698 (2009).
[17] I. I. Mazin, arXiv:condmat/0909.5174 (2009).
[18] X. Zhu, H. Yang, L. Fang, G. Mu, and H. H. Wen, Supercond. Sci. Technol. **21**, 105001 (2008).
[19] A. C. Larson, R. B. Von Dreele, General Structure Analysis System (GSAS), Los Alamos National Laboratory Report LAUR 86-748, (2004).
[20] N. R. Werthamer, E. Helfand, P. C. Hohenberg, Phys. Rev. **147**, 295 (1966).